TRACE METALS IN AIRBORNE PARTICULATE MATTER AND GENOMIC CHARACTERIZATION OF ASSOCIATED MICROORGANISMS

September 15, 2023

Center for Advancing Research in
Transportation Emissions, Energy, and Health
A USDOT University Transportation Center

Disclaimer

TECHNICAL REPORT DOCUMENTATION PAGE

1. Report No.	2. Government Accession No.	3. Recipient's Catalog No.
4. Title and Subtitle Trace Metals in Airborne Particulate Matter and Genomic Characterization of Associated Microorganisms: Insights into Health Effects from an Industrialized, Near-Roadway Site in Houston		5. Report Date September 2023 6. Performing Organization Code
7. Author(s) Shankar Chellam Alyvia K. McEwen Sourav Das		8. Performing Organization Report No. 03-25-TTI
9. Performing Organization Name and Address: CARTEEH UTC Department of Civil and Environmental Engineering College Station, TX 77843		10. Work Unit No. 11. Contract or Grant No. 69A3551747128
12. Sponsoring Agency Name and Address Office of the Secretary of Transportation (OST) U.S. Department of Transportation (USDOT)		13. Type of Report and Period Final January 2020 – December 2022 14. Sponsoring Agency Code

15. Supplementary Notes

This project was funded by the Center for Advancing Research in Transportation Emissions, Energy, and Health University Transportation Center, a grant from the U.S. Department of Transportation Office of the Assistant Secretary for Research and Technology, University Transportation Centers Program.

16. Abstract

This research simultaneously measured major/trace metals and microorganism diversity in airborne particulate matter ≤ 10 µm in aerodynamic diameter. The objectives were to (i) analyze the elemental composition of PM_{10}, (ii) perform source apportionment to quantify vehicular contributions, and (iii) implement state-of-the-art next generation sequencing tools to evaluate airborne microorganism diversity and prevalence. Filter samples were collected over a 9-day period spanning August 10–August 18, 2018, at Clinton Drive in Houston, Texas (latitude 29.73372; longitude −95.25759). Source apportionment modeling resolved vehicular emissions, resuspended local soil/road dust, and construction activities as major PM_{10} sources. Coincidentally, our sampling campaign captured a strong African dust event in Houston. Hence, all our results include a foreign component of aerosol mass, chemistry, and microbiology. Estimated vehicular emissions ranged between ~4.6–11.2 $\mu g/m^3$, averaging 7 $\mu g/m^3$. This constituted ~11 percent of the measured total PM_{10} mass on average. Estimated contributions from local soil and road dust were between ~8.0–28.5 $\mu g/m^3$, averaging 19.9 $\mu g/m^3$. This constituted ~31 percent of the measured total PM_{10} mass on average. Opportunistic human, plant, or animal pathogenic bacterial species were identified including *Escherichia coli, Propionibacterium acnes, Roseomonas mucosa,* and *Haemophilus parainfluenzae*. Several genera listed in the World Health Organization's (WHO's) global priority pathogens list of multidrug and antibiotic-resistant bacteria and tuberculosis were detected including *Acinetobacter, Enterococcus, Haemophilus, Mycobacterium, Pseudomonas,* and *Staphylococcus*. Fungi responsible for invasive human diseases such as *Aspergillus fumigatus, Fusarium* spp., and *Talaromyces* spp. that are listed as being priority pathogens for global public health by WHO appeared in nearly every sample along with all four most prominent allergenic fungal genera, viz. *Alternaria, Cladosporium, Aspergillus,* and *Penicillium*.

17. Key Words	18. Distribution Statement
PM_{10}, Elemental analysis, Airborne bacteria, Airborne Fungi, Bioaerosols	No restrictions. This document is available to the public through the CARTEEH UTC website. http://carteeh.org

19. Security Classif. (of this report)	20. Security Classif. (of this page)	21. No. of Pages	22. Price
Unclassified	Unclassified	31	$0.00

Form DOT F 1700.7 (8-72) Reproduction of completed page authorized

Executive Summary

Problem statement

Traffic related air pollution (TRAP) diminishes lung function, induces asthma, allergic rhinitis, respiratory infections, retards brain function, and stunts children's overall development [1-5]. Additionally, a high incidence of lung cancers, allergies, pulmonary and cardiovascular diseases, and premature death has been reported in populations living adjacent to highways and busy roadways [4]. Since particulate matter [6] mass concentrations are strongly correlated to morbidity and mortality [7, 8], a portion of the negative health impacts attributed to TRAP is assigned to inhalable particulate matter (PM). It is emphasized that causal correlations are well-accepted only for PM mass (not its specific constituents), justifying federal PM_{10} and $PM_{2.5}$ National Ambient Air Quality Standards based on daily or annual average mass concentrations (μg of PM per m^3 of air).

An important data gap in the existing literature is the detailed characterization of long-term exposure to lower levels of a wide range of vehicular metals that potentially lead to chronic health issues. In this research, we addressed this lack of rigorous information traffic related PM components by measuring concentrations of ~50 elements in vehicular emissions using mass spectrometry and then performing source apportionment modeling. Our measurements and calculations incorporate realistic estimates of primary tailpipe and non-tailpipe PM_{10} (particulate matter with aerodynamic diameters ≤ 10 μm) emissions under actual on-road conditions, including several real-world sources of variability such as maintenance histories, vehicle age, engine size and type, and driving habits that were obtained from measurements near a heavily trafficked roadway [9, 10].

Technical objectives, approach, and methodology

Our overarching objectives of this first comprehensive study designed to simultaneously measure major/trace metals and microorganism diversity in airborne coarse particulate matter were to:

- Quantify vehicular contributions to PM_{10} and associated human exposure by analyzing aerosols' elemental composition and perform source apportionment using the United States Environmental Protection Agency's Chemical Mass Balance (CMB v8.2) model.
- Implement state-of-the-art next generation sequencing tools to evaluate airborne microorganism diversity and prevalence in PM_{10} samples.

Filter samples were collected over a 9-day period spanning August 10–August 18, 2018, at Clinton Drive in Houston, Texas (latitude 29.73372; longitude −95.25759). This site is in a densely populated and economically depressed area (26.4 percent poverty rate) inhabited largely by ethnic minorities (91 percent Hispanics, African Americans, American Indians, and Alaska Natives) bringing environmental justice issues into focus. Clinton Drive is close to several heavily trafficked roads including Interstate-610 and Interstate-10, which had annual average daily traffic counts of 178,800 and 194,945 vehicles, respectively, and is within the Houston Ship Channel region, a hyper-industrialized section of the city. Therefore, air quality indices are frequently in the unhealthy range at this site, which consequently has been the target of many investigations [11-14].

One half of each filter was analyzed for elemental concentrations using high temperature microwave assisted acid digestion and inductively coupled plasma–mass spectrometry. The other half was used to quantify microorganism diversity by amplifying the V3 and V4 hypervariable regions of 16S ribosomal DNA (rDNA) and the highly variable internal transcribed spacer (ITS) region of rDNA (18S/ITS). Bioinformatics tools were used to identify the composition and abundance of prokaryotes and eukaryotes using 16S and 18S/ITS data, respectively.

Key findings

Source apportionment modeling resolved vehicular emissions, resuspended local soil/road dust, and construction activities as major PM_{10} sources. Coincidentally, our sampling campaign captured a strong African dust event in

Houston. Hence, all our results include a foreign component of aerosol mass, chemistry, and microbiology. The main findings from chemical mass balance modeling were:

- Measured ambient PM_{10} concentrations ranged between ~45–116 μg/m^3, averaging 73 μg/m^3.
- Estimated vehicular emissions ranged between ~4.6–11.2 μg/m^3, averaging 7 μg/m^3. This constituted ~11 percent of the measured total PM_{10} mass on average.
- Estimated contributions from local soil and road dust were between ~8.0–28.5 μg/m^3, averaging 19.9 μg/m^3. This constituted ~31 percent of the measured total PM_{10} mass on average.
- Estimated contributions from construction activities were between ~1.5–18.1 μg/m^3, averaging 6.3 μg/m^3. This constituted ~31 percent of the measured total PM_{10} mass on average.
- Estimated contributions from North African dust were between ~2.0–65.7 μg/m^3, averaging 24.5 μg/m^3. This constituted ~8.5 percent of the measured total PM_{10} mass on average.

The main findings from genomic sequencing of ambient PM_{10} were:

- Opportunistic human, plant, or animal pathogenic bacterial species were identified including *Escherichia coli*, *Propionibacterium acnes*, *Roseomonas mucosa*, and *Haemophilus parainfluenzae.* Several genera corresponding to human and plant pathogens were also detected.
- Several genera listed in the World Health Organization's (WHO) global priority pathogens list of multidrug and antibiotic-resistant bacteria and tuberculosis [15] were detected including *Acinetobacter*, *Enterococcus*, *Haemophilus*, *Mycobacterium*, *Pseudomonas*, and *Staphylococcus*.
- Fungi responsible for invasive human diseases such as *Aspergillus fumigatus*, *Fusarium* spp. and *Talaromyces* spp. that are listed as being priority pathogens for global public health by WHO [16] appeared in nearly every sample along with all four most prominent allergenic fungal genera, viz. *Alternaria*, *Cladosporium*, *Aspergillus*, and *Penicillium*.
- Numerous extremophilic and thermophilic genera of bacteria (*Chroococcidiopsis*, *Deinococcus*, *Hydrogenophilus*, *Meiothermus*, and *Saccharomonospora*) and fungi (*Alternaria*, *Aspergillus*, *Chaetomium*, *Cladosporium*, *Coprinopsis*, *Pencillium*, *Rhizopus*, *Scytalidium*, *Stemphylium*, *Talaromyces*, *Thanatephorus, Thermomyces*, *Thielavia,* and *Wallemia*) were identified [17].

Project Impacts

This research is a systematic and rigorous investigation that coupled primary PM_{10} sources, detailed elemental characterization, and DNA sequencing to provide essential information for animal, plant, and ecosystem health studies in a North American metroplex. We identified transportation sources, local industrial sources, and long-range transported dust from the Sahara-Sahel region impacting the chemical and microbiological composition of respirable aerosols in Houston, TX. We published our major findings in the journal *Environmental Science & Technology* [18]. Our outreach activities were geared towards informing elementary school students about environmental impacts of the transportation sector. Demonstrations performed for fourth graders familiarized them with direct (primary) emissions from motor vehicles, focusing their attention on environmental issues. This research addresses two of CARTEEH's priority areas: measurement and modeling, in the context of public health. Results from this short-term pilot-study provide the foundation for designing future investigations to better demarcate long-range transported microorganisms from locally aerosolized ones. Future research also needs to complement metagenomically identified bacteria and fungi by monitoring viability to better assess microorganisms' role in ecosystem and animal health.

Acknowledgments

Portions of this work were made possible with funding from the Texas Air Research Center. We appreciate the contributions of Dr. Daniel Spalink, Assistant Professor in the Department of Ecology and Conservation Biology, Texas A&M University, College Station, Texas, and Dr. Joseph Prospero, Emeritus Professor in the Department of Rosenstiel School of Marine and Atmospheric Science, University of Miami, Miami, Florida. Lauren James assisted with some of the outreach activities.

Table of Contents

List of Figures

List of Tables

Background and Introduction

Populations living adjacent to highways and busy roadways have an increased risk for morbidity and premature mortality [19-22] with reports of a high incidence of lung cancers, allergies, respiratory and cardiovascular diseases, and even premature death [23]. A portion of these health impacts has been assigned to airborne particulate matter [6] and its metals content [8, 19]. This necessitates detailed elemental characterization of vehicular particulate matter (PM) emissions and accurate identification and apportionment of ambient PM arising from motor vehicles. For these and other impacts of aerosols on human and ecosystem health [24-32], much research has focused on characterizing their chemical composition and epidemiological/toxicological effects to develop scientific policy enabling targeted emission control strategies to reduce their mass concentrations [31, 33, 34].

In addition to direct emissions, motor vehicles also resuspend soil and road dust that harbor microorganisms, indirectly emitting toxins into the local atmosphere, which may induce negative health impacts. In this research, we targeted PM_{10} to capture fungi and several other airborne microbes even though $PM_{2.5}$ and finer fractions penetrate deeper into the respiratory tract. One of the novelties of our research lies in the fact that in contrast to physical and chemical characterization of ambient aerosols, comparatively fewer reports have considered airborne microorganisms even though they also influence public health and the environment [17, 24, 35, 36].

For these reasons, we undertook a pilot study of aerosols enriched in metals and microorganisms. We focused on the city of Galena Park, which is adjacent to the Houston Ship Channel that serves the United States' largest petrochemical complex, the second busiest port by cargo volume, and myriad other concatenating industries. Galena Park is predominantly populated by Hispanics, African Americans, and Native Americans (92 percent) with a low per capita income (only $15,190) and high (26.4 percent) poverty rate [37]. Since air pollution exposure is skewed to low income and minority populations [38], our work also addressed environmental justice concerns [39-41]. Further, Houston is an interesting urban testbed to evaluate traffic related aerosols since Texas ranks second only to California in terms of vehicle miles traveled. Hence, the explicit focus of the work was to measure a wide suite of particulate metals and microorganism diversity in airborne PM_{10} at a busy intersection near the ship channel.

The overarching objectives of this first-of-its-kind study designed to simultaneously measure major/trace metals and microorganism diversity in airborne coarse particulate matter in North America were to:

- Collect ambient PM_{10} samples and quantify elemental concentrations using high temperature microwave assisted acid digestion and inductively coupled plasma–mass spectrometry (ICP-MS),
- Perform source apportionment using the United States Environmental Protection Agency's (EPA's) Chemical Mass Balance (CMB v8.2) model to determine the extent to which various sources including tailpipe and non-tailpipe emissions and resuspended road dust contributed to ambient PM_{10} concentrations,
- Implement state-of-the-art next generation sequencing tools to evaluate airborne microorganism diversity and prevalence in PM_{10} samples, and
- Develop outreach activities geared towards informing elementary school students about environmental impacts of the transportation sector.

Problem

As explained above, it is well recognized that traffic related air pollution causes a wide range of human health problems. Even though PM [6] regulations are mass based, it is well-accepted that metals are an important component that is responsible for the observed health end points. Hence, it is important to quantitatively estimate aerosols emitted by motor vehicles and evaluate their metals composition. An additional consideration is that although several studies have measured metals in airborne PM, comparatively fewer reports have considered airborne microorganisms even though they also influence public health and the environment.

Approach

We undertook a systematic and rigorous study to measure particulate metals and airborne microorganisms at a heavily trafficked intersection in greater Houston. Filter PM_{10} samples were collected over a 9-day period spanning August 10–August 18, 2018, at Clinton Drive in Houston, Texas (latitude 29.73372; longitude −95.25759). They were analyzed for metals using ICP-MS following high temperature microwave assisted acid digestion. This information was used to perform source apportionment to quantify PM emissions from motor vehicles, resuspended soil and road dust, and other local and global sources that influenced ambient aerosol concentrations. Bacterial and fungal diversity were quantified by amplifying the V3 and V4 hypervariable regions of 16S ribosomal DNA (rDNA) and the highly variable internal transcribed spacer (ITS) region of rDNA (18S/ITS).

Methodology

PM_{10} sampling

A ThermoFisher 2025i Partisol sequential air sampler was used to collect samples on PTFE filters. All sampler parts (i.e., inlets, filter cassettes, filter cartridge, carrier box support, and filters) were disinfected with 70 percent ethyl alcohol followed by 5 percent hypochlorite solution. Filters were disinfected by exposing them to UV light for 15 minutes inside a biosafety cabinet (Baker SterilGARD, Class II Type A2). Filters were refrigerated at −80°C immediately after removing from the sampler (using sterile tweezers), weighed to measure PM_{10} mass concentrations, cut into two halves using a sterilized ceramic knife inside a biosafety cabinet (one for elemental analysis and the other for sequencing), and again stored at −80 °C in sterile petri dishes until further analysis.

Elemental analysis

The filter half designated for elemental analysis was digested first in 3 mL of trace metal grade concentrated HNO_3 with additional optima grade concentrated HF in a ratio of 0.3 mL for every 10 mg of sample, based on our previous work [12, 13, 42, 43]. This was followed by adding 5 percent w/v boric acid solution to mask the insoluble fluoride complexes and was re-digested. Each stage was performed at 200°C and 200 psig in a microwave oven (MARS 6, CEM Corporation) for a dwell time of 20 min. The digested aliquot was then diluted to 2 percent nitric acid matrix before analyzing with ICP-MS. The 46 elements were measured including 31 from Groups 1–16 (Na, Mg, Al, Si, K, Ca, Sc, Ti, V, Cr, Mn, Fe, Co, Ni, Cu, Zn, Ga, As, Se, Rb, Sr, Zr, Mo, Cd, Sn, Sb, Cs, Ba, Pb, Th, and U) and 15 rare earths (Y, La, Ce, Pr, Nd, Sm, Eu, Gd, Tb, Dy, Ho, Er, Tm, Yb, and Lu). Al, V, Cr, Fe, Ni, Cu, and Zn were analyzed in Dynamic Reaction Cell mode using ammonia as the cell gas to reduce polyatomic interferences [12, 42-45].

Nucleic acid extraction and gene sequencing

Nucleic acids were extracted from the Teflon filters using bead-beating and purification with centrifugal filters. PM_{10} filters were cut in half, folded with sterile forceps, and placed into 2-mL bead beating tubes (National Scientific supply, BC20NA-PS), along with 200 mg of ≤ 106 µm diameter glass beads (Sigma, G-4649), 200 mg of 425–600 µm glass beads (Sigma, G-8772), and 650 µL of sodium phosphate buffer prepared aseptically by mixing 1.0 µL Tween 20 with 10 ml of 0.1 M sodium phosphate/10 mM EDTA (Teknova, Hollister, CA). The bead beating tube was mechanically disrupted with a mini-bead beater (BioSpec Products, Bartlesville, OK) for 3 min at 3450 oscillations/min and subsequently placed on ice for 5 min. After cooling, tubes were centrifuged at 7000×g for 2 min. 500 µL of supernatant was transferred to a Ultrafree-MC centrifugal filter (0.22 µm pore size, hydrophilic PVDF, 0.5 mL volume, UFC30GV0S) and centrifuged at 10,000×g for 3 min. Following the centrifugal pre-filtration, the filtrate was transferred to an Amicon Ultra-0.5 (100,000 Molecular Weight Cut-Off) centrifugal filter device

(YM-100, Millipore) and centrifuged for 3 min at 7000×g. This step concentrated nucleic acids on the filter while allowing inhibitory compounds to pass through. The filter was first washed twice, each time by adding 200 µL of TE buffer to the retentate cup and centrifuging for 3 min at 7000×g. After the second wash, 100 µL of the TE was added and centrifuged for 1 min at 7000×g and subsequently in 10 second pulses as needed to recover 100 µL through the filter. Nucleic acids were recovered from the top of the Amicon filter insert by inverting the filter into a fresh tube by centrifugation at 1000×g for 2 min. Final purification of nucleic acids was performed as per manufacturer's protocol using a polyvinylpolypyrrolidone spin column (Spin-IV-HRC, Zymo Research).

We followed the protocol recommended by Swift Biosciences to generate amplicons that cover all variable regions of the 16S rDNA, ITS1, and ITS2 genes in a single primer pool using the Swift Amplicon 16S + ITS kit. The PCR products (obtained following their protocol) were cleaned up using the Agencourt AMPure XP beads (Beckman Coulter Genomics), and the purified amplicon was resuspended in 25 µl TE buffer. The first round of purified amplicon was amplified using the Illumina adaptors specific dual indexed Nextera XT barcoded primers of index 1 (i7) adapter and index 2 (i5) adapter with 15 cycles of amplification followed by clean-up. The amplicons were purified with Agencourt AMPure XP beads, quantified with Qubit (Invitrogen), and verified the amplicon size with Agilent TapeStation 2200 system. The library pool was diluted to obtain a final concentration of 8 pM. The 600 µL of the library pool was loaded on to a MiSeq v2 reagent cartridge (500 cycle v2 kit) and 251 bp paired-end sequencing protocol (2×251 cycles) was performed on MiSeq platform (Illumina).

Raw sequence reads were cleaned and processed using QIIME v1.9.1 [46]. Forward and reverse reads were merged, assigned to samples according to barcodes, and then trimmed to remove barcode and primer sequences. Sequences shorter than 200 bp, those containing ambiguous bases, and those with mean quality scores of < 20 were discarded. The remaining sequences were then aligned to the reference UCHIME RDP 'Gold' database to identify and remove chimera sequences. Sequence reads were clustered into Operational Taxonomic Units (OTUs) using VSEARCH v.1.9.6[47] and the SILVA 119 database[48] for 16s and the UNITE database for ITS[49]. For both gene regions, sequences were assigned to OTUs using a 0.8 threshold, with taxonomic categories parsed up to the species level, and subsequently rarified prior to downstream analyses.

Source apportionment

EPA's Chemical Mass Balance (CMB v8.2) model was employed to quantify contributions of various sources to PM_{10} mass concentrations [12, 13, 50, 51]. Na, Mg, Si, K, Ca, Ti, Co, Cu, As, Se, Sr, Sn, Sb, Mo, Ba, Pb, Al, V, Cr, Fe, Ni, Zn, Y, La, Ce, Pr, Nd, and Sm were chosen as fitting species based on their importance as elemental tracers and level of uncertainty in our laboratory measurements. Sb, Cu, Cd, Sn, Pb, Mo, As and Zn were selected as traffic-related metals [43, 51, 52]; Zn, Pb, Cr, Mn, Mg, Co, and Ni were selected to track high-temperature industrial processes [45]; rare earths (La, Ce, Nd, Pr, Sm, Gd, and Eu) were chosen for petroleum refining (fluidized bed catalytic cracking) activities and crustal matter [14, 43, 44]; V and Ni were chosen for oil combustion and shipping activities [53, 54]; and Al, Si, Ti, Ca, Fe and Y were used to isolate crustal mass [13, 43].

Results

Overall trends in PM_{10} and $PM_{2.5}$ mass

Details of the nine daily PM_{10} samples (labelled S1–S9) collected are given below in Table 1. $PM_{2.5}$ concentrations that were measured at the same location by the Texas Commission on Environmental Quality (TCEQ) are also included.

Table 1. Summary of sampling, aerosol mass concentrations, and the two transportation-related sources.

Sample ID	Start date	End date	PM_{10} ($\mu g/m^3$)	$PM_{2.5}$† ($\mu g/m^3$)	Apportioned vehicular emissions ($\mu g/m^3$)	Apportioned local soil and road dust emissions ($\mu g/m^3$)

S1	10 Aug	11 Aug	44.7	12.2	8.91	23.3
S2	11 Aug	12 Aug	51.7	19.8	4.55	11.4
S3	12 Aug	13 Aug	115.7	37.9	6.92	14.9
S4	13 Aug	14 Aug	104.7	30.7	3.63	22.9
S5	14 Aug	15 Aug	98.3	22.2	8.36	20.9
S6	15 Aug	16 Aug	64.6	13.7	6.86	20.6
S7	16 Aug	17 Aug	74.4	13.9	11.2	28.3
S8	17 Aug	18 Aug	55.2	11.3	7.72	8.1
S9	18 Aug	19 Aug	45.1	9.3	4.95	28.5

† Measured by the Texas Commission on Environmental Quality (TCEQ).

As summarized in Table 1, $PM_{2.5}$ and PM_{10} exhibited similar trends increasing ~3-fold from the first sample (S1) to the third sample (S3) before progressively declining to routine levels in the last sample (S9). The $PM_{2.5}$ level was 37.9 µg/m^3 in sample S3, which is more than three times the annual average primary standard of 12 µg/m^3 established by EPA. The average $PM_{2.5}$ concentration throughout this sampling period was 19 µg/m^3, which is 58 percent higher than EPA's annual average primary National Ambient Air Quality Standard (NAAQS). It even exceeded the primary and secondary 24-hour NAAQS standard of 35 µg/m^3. PM_{10} never exceeded the 24-hour primary and secondary NAAQS but approached the limit of 150 µg/m^3 in sample S3. PM_{10} averaged 72 µg/m^3 over the study period.

Trends in elemental concentrations

Figure 1 summarizes elemental concentrations in PM_{10} over the study duration. As seen, elemental concentrations varied over nearly seven orders of magnitude (e.g., from 2 pg/m^3 for thulium and lutetium in samples S1 and S9 to 18 µg/m^3 for silicon in sample S5). The large variability in elemental composition is attributed to the inherently high variability associated with PM sources in greater Houston [13, 14, 55-58].

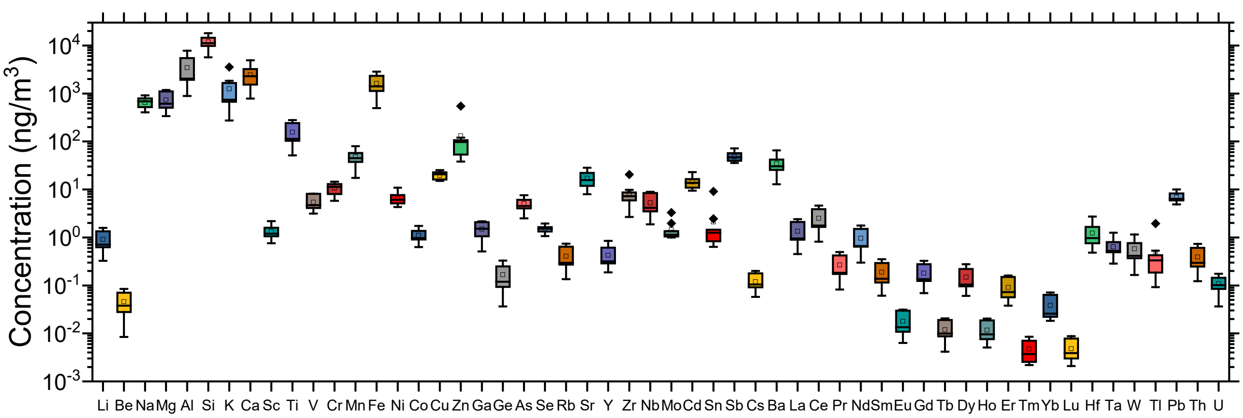

Figure 1. Box plot of elemental concentrations in PM_{10} over the study duration. The box encompasses the 25% and 75% percentiles, the whiskers span 1.5 times the interquartile range, and outliers are shown as diamonds. Inside each box, the horizontal line is the median value and the hollow square symbol (□) is the average value.

Crustal elements (e.g., Na, Mg, Al, Si, Ca, Ti, and Fe) dominated in aerosols, suggesting that aeolian resuspension was their important source. Importantly, rare earth elements (REEs) were consistently detected, which exhibited abundances following the Oddo–Harkins rule with even atomic numbered REEs being more abundant than their immediate neighbors with odd atomic numbers except for samarium anomalies (i.e., La < Ce > Pr < Nd > Sm > Eu < Gd > Tb < Dy > Ho < Er > Tm < Yb > Lu). This trend validated the importance of crustal material as a dominant source of aerosols during the study period. Numerous main group (e.g., Li, Be, Ga, As, Sn, Sb, and Pb) and transition metals (e.g., V, Cr, Co, Ni, Cu, Zn, Mo, and Cd) were detected, many of which are known air toxics.

Source apportionment

Chemical Mass Balance (CMB) modeling estimated North African dust as the dominant source during the sampling campaign contributing 29 ± 22 percent (7–57 percent) over the study duration. Other local sources quantified included resuspended local soil/road dust as the second most dominant source, contributing 31 ± 16 percent (13–63 percent) over the study duration. Both these are predominantly derived from crustal materials, validating the observations made in the previous section regarding aeolian resuspension of aerosols. Construction activities and vehicular emissions also had significant impacts averaging 9 ± 6 percent (3–24 percent) and 11 ± 5 percent (3–20 percent), respectively. Although oil combustion modified vanadium atmospheric chemistry as described in the previous section, it contributed only negligibly to PM_{10} mass 0.18 ± 0.25 percent (0–0.8 percent). Sea salt was another minor contributor to mineral matter, contributing an average of 2.3 ± 3.8 percent (0–9.7 percent). The relevant source contribution estimates from CMB modeling are summarized in Figure 2.

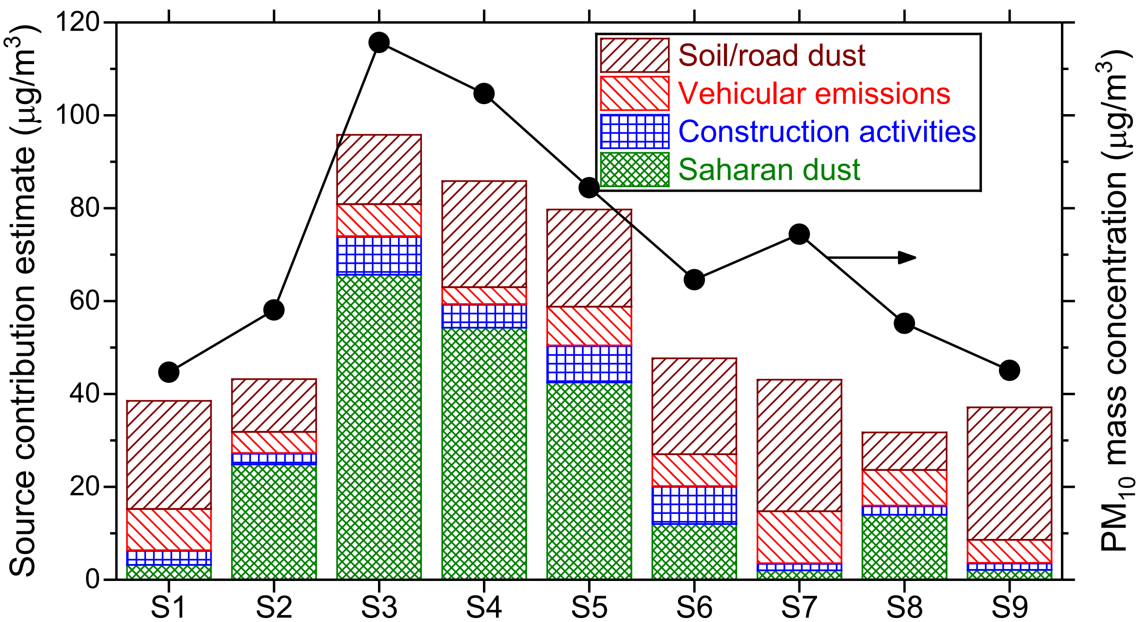

Figure 2. Chemical mass balance modeling results for daily samples (S1–S9) depicting relevant source contribution estimates. Vehicular emissions are shown in red hatches and construction activities are depicted in blue hatches.

Bacterial community structure

Following quality control, 16S rDNA gene sequencing generated an average of 30,981 reads per sample, varying between 2,005 and 65,154 reads. There were 848 bacterial OTUs recorded over the sampling campaign, representing 17 phyla, 46 classes, 117 families, and 121 genera.

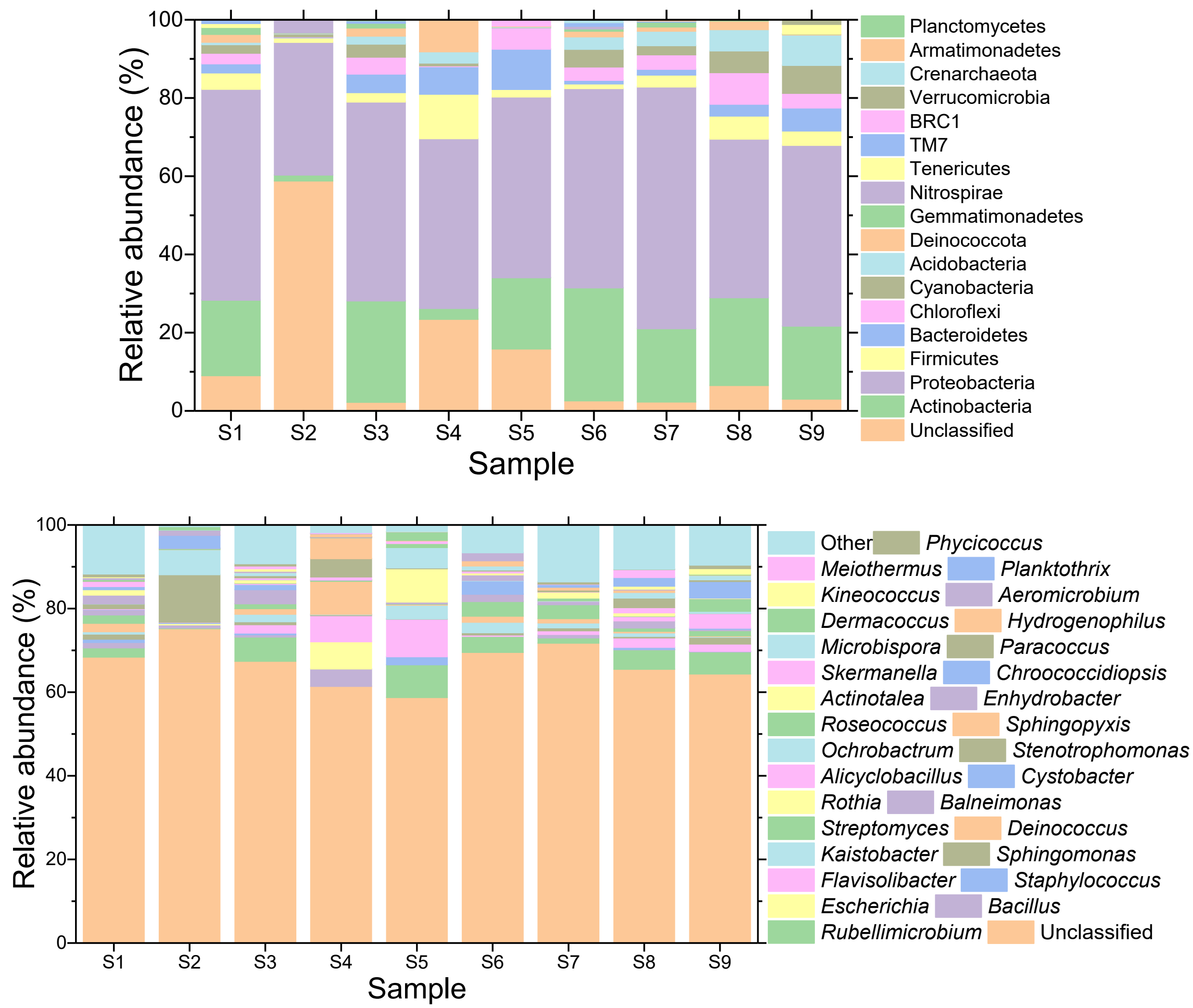

Figure 3. (Top panel) The relative abundances of bacterial phyla over the nine-day sampling campaign. (Bottom Panel) The relative abundances of the top 30 bacterial genera, including the portion of reads unable to be classified to the genus level (Unclassified) and other, over the nine-day sampling campaign.

Fungal community structure

ITS rDNA gene sequencing resulted in a mean of > 109,000 counts per sample, which was significantly higher and less variable than that of bacteria. A total of 1345 fungal OTUs were identified, representing 4 phyla, 20 classes, 69 orders, 164 families, and 286 genera.

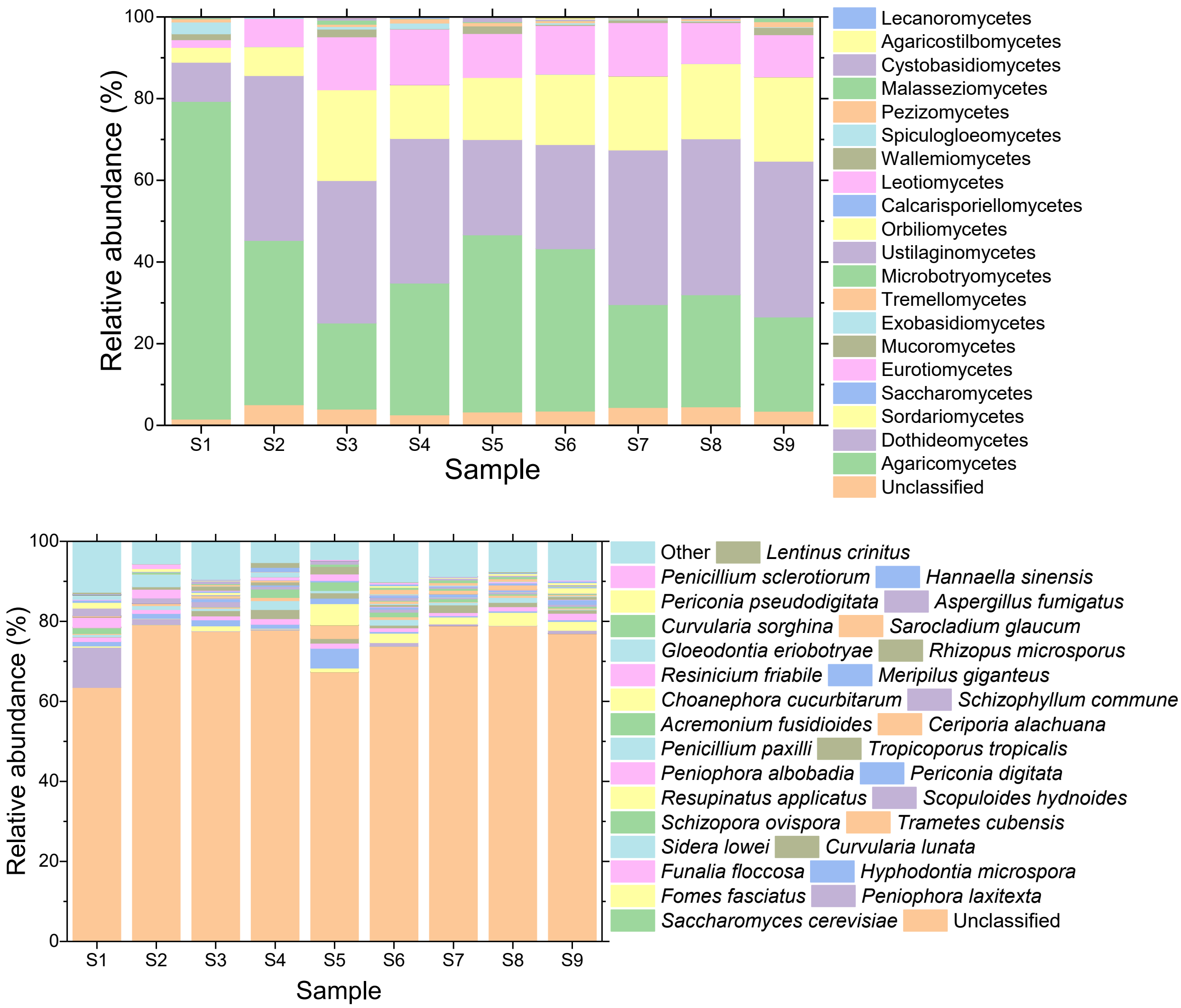

Figure 4. (Top panel) The relative abundances of fungal classes over the nine-day sampling campaign. (Bottom panel). The relative abundances of the top 30 fungal species, including the portion of reads unable to be classified to the species level (Unclassified) and other, over the nine-day sampling campaign.

Potential human and environmental health impacts

The study of bioaerosols has become increasingly popular in recent years as scientists look not only at genetic but environmental risk factors for conditions like asthma, respiratory ailments, and certain cancers. Suspended bacterial and fungal cells that can maintain viability throughout short or long-distance transport can impact the surrounding climate, human health, plant health, animal health, atmospheric chemistry, and ecology.

Fungi responsible for invasive human diseases such as *Aspergillus fumigatus*, *Fusarium* spp. and *Talaromyces* spp. that are listed as being priority pathogens for global public health by WHO [16] appeared in nearly every sample along with all four most prominent allergenic fungal genera, viz. *Alternaria*, *Cladosporium*, *Aspergillus*, and *Penicillium* [59]. Their total relative abundance peaked in S3, the date of highest dust loading (Figure 5). Fungi form spores more readily than bacteria, resulting in their greater potential to remain viable even after exposure to wind and UV light when suspended. Because of their heightened durability, their potential impact to human health is emphasized.

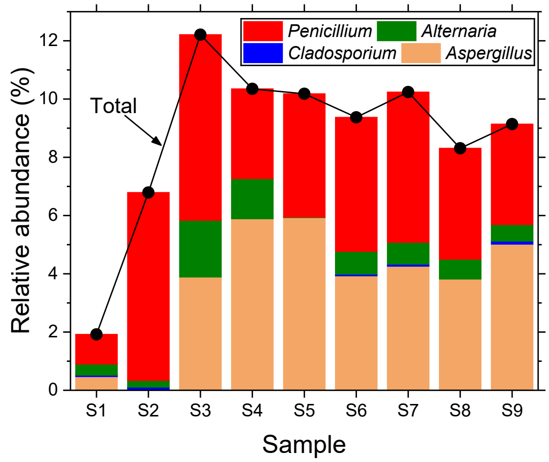

Figure 5. Four prominent allergenic fungal genera and their relative abundances spanning the nine-day sampling campaign.

Numerous genera of plant or human pathogenic fungi including *Cercospora*, *Curvularia*, *Flavodon*, *Fomes*, *Fuscoporia*, *Funalia,* and *Magnaporthe* were also detected. Several pathogenic species peaked in abundance synchronous with North African dust including *Curvularia lunata*, *Rhizopus microsporus*, *Penicillium sclerotiorum, Phellinus gilvus, Exserohilum rostratum*, *Aureobasidium pullulans,* and *Curvularia trifolii*. We also detected saprobic fungi that play a critical role in carbon cycling such as *Basidiomycota*, *Neurospora*, *Peniophoraceae*, and the species *Phanerochaete chrysosporium* and *Trametes versicolor*.

Opportunistic human, plant, or animal pathogenic bacterial species were identified including *Escherichia coli*, *Propionibacterium acnes*, *Roseomonas mucosa*, and *Haemophilus parainfluenzae*. Several genera listed in WHO's global priority pathogens list of multidrug and antibiotic-resistant bacteria and tuberculosis [15] were detected including *Acinetobacter*, *Enterococcus*, *Haemophilus*, *Mycobacterium*, *Pseudomonas*, and *Staphylococcus*. Other pathogens measured included the Gram negative *Achromobacter*, *Caulobacter*, *Chitinophaga*, *Chryseobacterium*, *Clostridium*, *Corynebacterium*, *Gordonia*, *Listeria*, *Megasphaera*, *Nocardioides*, *Ochrobactrum*, *Propionivibrio*, *Sphingomonas*, *Stenotrophomonas*, and *Williamsia*, and the Gram positive *Actinomyces*, *Bacillus*, *Micrococcus*, *Nocardioides*, *Propionibacterium*, *Roseomonas*, and *Rothia*. The plant pathogens *Erwinia, Rhizobium* (a nitrogen fixer), and *Streptomyces* as well as the filamentous cyanobacterium *Planktothrix* capable of seeding harmful algal blooms were also detected.

(Poly)extremophilic and thermophilic genera of bacteria (*Chroococcidiopsis*, *Deinococcus*, *Hydrogenophilus*, *Meiothermus*, and *Saccharomonospora*) and fungi [60] (*Alternaria*, *Aspergillus*, *Chaetomium*, *Cladosporium*, *Coprinopsis*, *Pencillium*, *Rhizopus*, *Scytalidium*, *Stemphylium*, *Talaromyces*, *Thanatephorus, Thermomyces*, *Thielavia,* and *Wallemia*) were also present.

An incomplete list of the potential pathogens noted in our dataset is included in Table 2 and Table 3 below.

Table 2. Bacterial species present in the samples with potential pathogenicity.

Species	Average Abundance	Impact	Description
Escherichia coli	0.76%	Animal Human	Avian pathogen Human intestinal pathogen
Propionibacterium acnes	0.16%	Human	Opportunistic: acne vulgaris, endocarditis, endophthalmitis, prosthetic joint infections
Roseomonas mucosa	0.05%	Human	Opportunistic/nosocomial infector: peritonitis, bacteremia, endocarditis, endophthalmitis
Haemophilus parainfluenzae	0.02%	Human	Opportunistic: upper respiratory tract infections, urogenital infections, gastroenteritis, endocarditis

Table 3. Fungal species identified in the dataset with potential pathogenicity.

Species	Average Abundance	Impact	Description
Fomes fasciatus	1.38%	Plant	Wood decay
Funalia floccosa	1.14%	Plant	White rot
Curvularia lunata	1.03%	Plant Human	Tomato early blight, leaf spot Phaeohyphomycosis
Tropicoporus tropicalis	0.49%	Plant Human	White rot Keratitis, Mycosis
Schizophyllum commune	0.38%	Plant	Wood rot
Choanephora cucurbitarum	0.37%	Human Plant	Lung infection Seedling rot, blight, fruit rot, leaf wilt, flower rot, stem necrosis, leaf spot
Rhizopus microsporus	0.33%	Human	Rhinocerebral mucormycosis, lung infection
Aspergillus fumigatus	0.29%	Human Animal	Aspergillosis Aspergillosis
Penicillium sclerotiorum	0.26%	Plant	Leaf spot, post-harvest decay
Phellinus gilvus	0.17%	Plant	Wood decay

Exserohilum rostratum	0.15%	Plant Human	Leaf spot, rice brown spot, lettuce root rot Sinusitis, Keratitis
Stemphylium herbarum	<0.1%	Plant	Brown spot, leaf spot
Penicillium sumatraense	<0.1%	Plant	Post-harvest decay
Aureobasidium pullulans	<0.1%	Human	Opportunistic: subcutaneous phaeohyphomycosis, fungemia, peritonitis, pneumonia
Fusarium oxysporum	<0.1%	Plant Human	Stem rot, wilt, dieback Fusariosis
Phanerochaete chrysosporium	<0.1%	Plant	White rot
Amphobotrys ricini	<0.1%	Plant	Gray mold
Penicllium georgiense	<0.1%	Plant	Post-harvest decay
Curvularia trifolii	<0.1%	Plant	Blight, leaf spot
Cladosporium sphaerospermum	<0.1%	Plant Human	Leaf spot Opportunistic: abscesses, cutaneous infections
Tilletia barclayana	<0.1%	Plant	Rice/grain smut
Hyphodermella rosae	<0.1%	Plant	White rot, dry fruit rot
Nigrospora oryzae	<0.1%	Plant	Leaf spot, leaf blight
Aurantiporus fissilis	<0.1%	Plant	Wood decay
Purpureocillium lilacinum	<0.1%	Human Animal	Opportunistic: hyalohyphomycosis, ocular infections Nematicide
Wallemia sebi	<0.1%	Human	Subcutaneous phaeohyphomycosis
Trichothecium roseum	<0.1%	Plant	Fruit rot, post-harvest decay, root rot, dieback, leaf spot
Periconia macrospinosa	<0.1%	Plant	Leaf necrosis

Aspergillus penicillioides	<0.1%	Human	Opportunistic: subcutaneous infections, keratomycosis, aspergillosis
Pilidium concavum	<0.1%	Plant	Tan-brown rot, fruit rot, leaf necrosis
Saccharomyces cerevisiae	<0.1%	Human	Opportunistic in immunocompromised patients: vaginitis, blood stream infections, essential organ infections
Eutypa leptoplaca	<0.1%	Plant	Grapevine pathologies; dieback
Rhizopus arrhizus	<0.1%	Plant Human	Root rot, soft rot, post-harvest rot Rhinosinusitis mucormycosis
Favolus grammocephalus	<0.1%	Plant	White rot
Biatriospora mackinnonii	<0.1%	Human	Eumycetoma, cutaneous phaeohyphomycosis
Gjaerumia minor	<0.1%	Human	Keratitis
Antrodia pini-cubensis	<0.1%	Plant	Brown rot
Trametes versicolor	<0.1%	Plant	White rot
Punctularia strigosozonata	<0.1%	Plant	White rot
Tolypocladium inflatum	<0.1%	Animal	Insecticidal
Monocillium indicum	<0.1%	Animal	Lymphadenitis, splenitis
Quambalaria cyanscens	<0.1%	Plant	Smut
Cordyceps bassiana	<0.1%	Animal	Insecticidal
Trichaptum abietinum	<0.1%	Plant	Wood decay
Thermomyces lanuginosus	<0.1%	Human	Opportunistic: endocarditis
Malassezia restricta	<0.1%	Human	Opportunistic: endocarditis, pneumonia, dermatitis
Bjerkandera adusta	<0.1%	Human	Bronchopulmonary mycosis
Waitea circinata var. circinata	<0.1%	Plant	Brown ring patch
Phlebia chrysocreas	<0.1%	Plant	Heartrot

Neopestalotiopsis foedans	<0.1%	Plant	Leaf spot
Phlebiopsis gigantea	<0.1%	Plant	Wood decay
Ceratobasidium ramicola	<0.1%	Plant	Dieback, leaf blight, leaf rot, damping off, root rot
Rigidoporus ulmarius	<0.1%	Plant	White rot
Postia caesia	<0.1%	Plant	Brown rot
Exidia glandulosa	<0.1%	Plant	Wood decay
Botryosphaeria dothidea	<0.1%	Plant	Blueberry canker, brown rot, pear ring rot, kiwi soft rot
Gonatobotryum apiculatum	<0.1%	Plant	Leaf spot, blight
Fibroporia radiculosa	<0.1%	Plant	Wood decay, brown rot
Daldinia eschscholtzii	<0.1%	Plant	Wood decay
Gloeophyllum trabeum	<0.1%	Plant	Wood decay, brown rot
Thanatephorus cucumeris	<0.1%	Plant	Rice sheath blight, tomato seedling damping off, potato black scurf, stem canker, root rot
Phaeoacremonium croatiense	<0.1%	Plant	Citrus tree diseases

Conclusions and Recommendations

Although we were able to quantify transportation through chemical analyses, microbiome composition was not as clear an indicator for particulate matter sourcing, potentially due to the ubiquity of certain microorganisms in the environment and limitations in genetic sequencing and identification. Our sampling campaign was incidentally overwhelmed by African dust and was fraught with multiple sources of particulate matter, making it difficult to exclusively assign microbial findings to the transportation sector.

Future studies should involve longer time-scales including when regional sources dominate aerosol composition in Houston. Furthermore, assessing viability (culturability) of microorganisms present in air samples is needed to better gauge the impact to ecosystem and human health.

Outputs, Outcomes, and Impacts

It is important to recognize that our sampling campaign unexpectedly coincided with a large African dust event. Although our primary objective was to determine emissions from the transportation sector, we also captured the role of long-range transported dust on PM_{10} levels along with its elemental and microbiological composition. Since this was a relatively "fundamental" research effort (i.e., not oriented towards technology development), our findings are not directly amenable for technology transfer. Having said that, our sampling, elemental analysis, and microbial sequencing and interpretation tools can be applied to other studies of transportation aerosols. Some important take home messages were deduced, as itemized below.

Research Outputs, Outcomes, and Impacts

- A manuscript based on these data has been published after peer-review: Sourav Das, Alyvia McEwen, Joseph Prospero, Daniel Spalink, and Shankararaman Chellam (2023). *Respirable Metals, Bacteria, and Fungi during a Saharan-Sahelian Dust Event in Houston, Texas*. Environmental Science & Technology, https://doi.org/10.1021/acs.est.3c04158 [18].

Technology Transfer Outputs, Outcomes, and Impacts

- This is the first of its kind North American dataset simultaneously characterizing a wide suite of metals and microbial (bacterial and fungal) diversity in respirable PM.
- Because we captured Saharan dust, our work has findings that have broader implications for microbial ecology associated with long-distance dispersal, Earth's radiation budget, climate, hydrology, and public health.
- Several metals and pathogenic microorganisms were present at elevated levels at a busy intersection, demonstrating increased human exposure to airborne toxics at this location. Cumulatively, direct vehicular emissions and resuspended soil/road dust contributed about 40 percent of the measured respirable PM mass. These findings can be extrapolated to other heavily trafficked intersections suggesting direct links between the portion of respirable PM arising from transportation and human health.
- Importantly, metagenomically identified bacteria and fungi do not imply that they are viable. Hence, future research needs to complement our preliminary findings by monitoring viability (culturability) to better assess microorganisms' role in ecosystem and animal/human health.
- Lesson plans communicated to elementary school students inculcated interest in environmental issues related to the transportation sector.

Education and Workforce Development Outputs, Outcomes, and Impacts

Our undergraduate students coordinated multiple outreach activities regarding traffic-related air pollution to elementary and high school students throughout the project duration with mentorship from Dr. Chellam.

Camp BUILD

On the weekend of January 15, 2022, two of our undergraduate assistants, Alyvia McEwen and Elisabeth Gerstacker, helped lead an air pollution demonstration for Camp BUILD. Camp BUILD is a Zachry Department of Civil and Environmental Engineering initiative created to familiarize high school upperclassmen with basic engineering concepts, the Texas A&M University campus, and Civil and Environmental Engineering faculty. Camp BUILD places an emphasis on reaching first-generation college students and engineers from underserved school districts across Texas. Over the weekend, 20 high school students participated in campus tours, admissions presentations, and hands-on demonstrations covering each of the subdisciplines within civil engineering, including the demonstration prepared by our team.

For the experiment, a candle was lit, placed in front of an air hose, and extinguished. Students were positioned 1 meter downstream of the candle with a PM monitor, and they recorded PM_{10} values using a handheld PM monitoring device at indicated time intervals for two minutes past when the candle was extinguished. The procedure was then repeated for a measurement of 2 meters downstream. Students divided out the necessary responsibilities including equipment manager, timekeeper, and data collector. For the demonstration, students were divided into teams of five, which allowed everyone to take ownership of the experiment and practice multiple roles. After all groups had taken the measurements, the students were tasked with graphing the PM_{10} levels over time for both configurations and comparing results.

Students seemed to enjoy seeing how seemingly invisible pollutants, a light smoke trail from the candle, evoked a dramatic response from the PM monitor, even at short times and large distances away from the source. They could see the numbers climbing on the PM monitor and hear the alarms progressing from a low to moderate hazard, to unhealthy for sensitive groups, then to severe hazard. It was stressed to the students that the burning candle represented larger-scale sources of incomplete combustion, including tailpipe emissions from vehicles. Students understood that residential areas close to busy highways or manufacturing facilities will experience different air quality issues than residential areas in more protected settings. This was presented as one of the reasons for erecting walls and planting trees in neighborhoods near highways (i.e., to physically exclude particulate matter). We discussed the differences between point and nonpoint sources of air pollution and noted that the students' graphs showed how air quality changes depending on distance from a point source and time since its emission. Overall, the outreach activity served to introduce environmental engineering as an important field of study to incoming first-generation college students, as well as provide teaching experience for our undergraduate assistants who are considering graduate studies.

Figure 6. (Top panel) Students take PM_{10} measurements at directed time and distance intervals after extinguishing a candle. (Bottom panel) Students work in teams to translate data into a graph of PM_{10} concentrations over time.

Southwood Valley Elementary School

On April 13, 2022, Alyvia McEwen and Sorya Meyer demonstrated air pollution experiments to the fourth-grade students at Southwood Valley Elementary School in College Station. Most students enrolled in this elementary school (61 percent) are underrepresented minorities and nearly the same percentage (55 percent) of the student body is classified as economically disadvantaged by the Texas Education Agency, ensuring that our STEM-related experiments reached a diverse set of students. We performed two 90-minute presentations in the cafeteria to all fourth graders who were present numbering approximately 100 students and 5 teachers.

The first demonstration was designed to show how motor vehicles contribute to air pollution through tailpipe emissions. In this experiment, several candles were placed among groups of students, each representing fossil fuel combustion in an internal combustion engine. A handheld PM monitor was used to first record the ambient concentrations within the school cafeteria before lighting the candles. For each PM reading, we let a few students take the monitor and read out the $PM_{2.5}$ and PM_{10} measurements as well as the monitor's built in health indicator ("good," "moderate," "unhealthy for sensitive groups," "unhealthy," "very unhealthy," and "hazardous"). Students took note that in the absence of burning candles, the cafeteria's indoor air was deemed "good." Next, students were instructed to ignite each candle, which acted as a surrogate for (incomplete) fuel combustion in an engine and a source for aerosols. Other students volunteered to extinguish the candle, and students reacted to the burnt smell and the visible trail of soot emitting from the wick. Students used the PM monitor to see how the indoor air quality changed after lighting the candle at varying distances from the source. They personally documented increasing $PM_{2.5}$ and PM_{10} concentration values soon after extinguishing the candles, which triggered the monitor's built-in alarm when aerosol levels reached "hazardous" levels close to the source. Students were fascinated by how drastically the particulate matter concentrations rose in a short period of time after the candle was burned and extinguished. They were able to connect increasing aerosol levels from the burning candle to gasoline and diesel combustion in motor vehicles. Additionally, we explained to the students based on these measurements how vehicles are a major contributor to poor air quality especially in large cities with poor public transportation systems and consequently that are highly dependent on private vehicles like many in Texas.

The second demonstration covered the topic of particle resuspension by vehicles (i.e., non-tailpipe emissions). To illustrate this, a small patch of the floor was covered with flour, leaves, soil, and other debris. Then, students volunteered to help drive an RC car back and forth over the patch. The students were able to watch the flour and debris get kicked up into the air by the RC car tires. They were able to understand that microscopic particles can be similarly resuspended by less intense motions, such as walking or even rubbing their hands together, and they were also able to consider how many particles are resuspended by heavy traffic. In both demonstrations, it was emphasized to the students that our air quality is affected daily by industry and traffic, and it has health consequences for people that live or work in locations closest to the pollutant sources. At the end of our demonstrations, students were asked to share what they learned, and their responses showed excitement and appreciation that STEM knowledge (with engineering applications) could tackle transportation and environmental issues that affect real people every day.

Figure 7. (Left panel) Students measure PM levels near a lit candle. (Middle panel) Students recognize an increase in PM levels after the candle is extinguished. (Right panel) Volunteers drive the remote-controlled car over the flour patch as they visualize tires kicking up particles.

Navarro Elementary School

On October 17, 2022, Alyvia McEwen, Sorya Meyer, and Elisabeth Gerstacker outreached to roughly 75 students at Navarro Elementary School in Bryan, Texas. About 35 percent of the student body has limited English proficiency, and roughly 88 percent of the students are classified as economically disadvantaged. The same two demonstrations from the Southwood Valley Elementary School outreach were performed for the three fourth-grade classes at Navarro, including one class of English as a Second Language students.

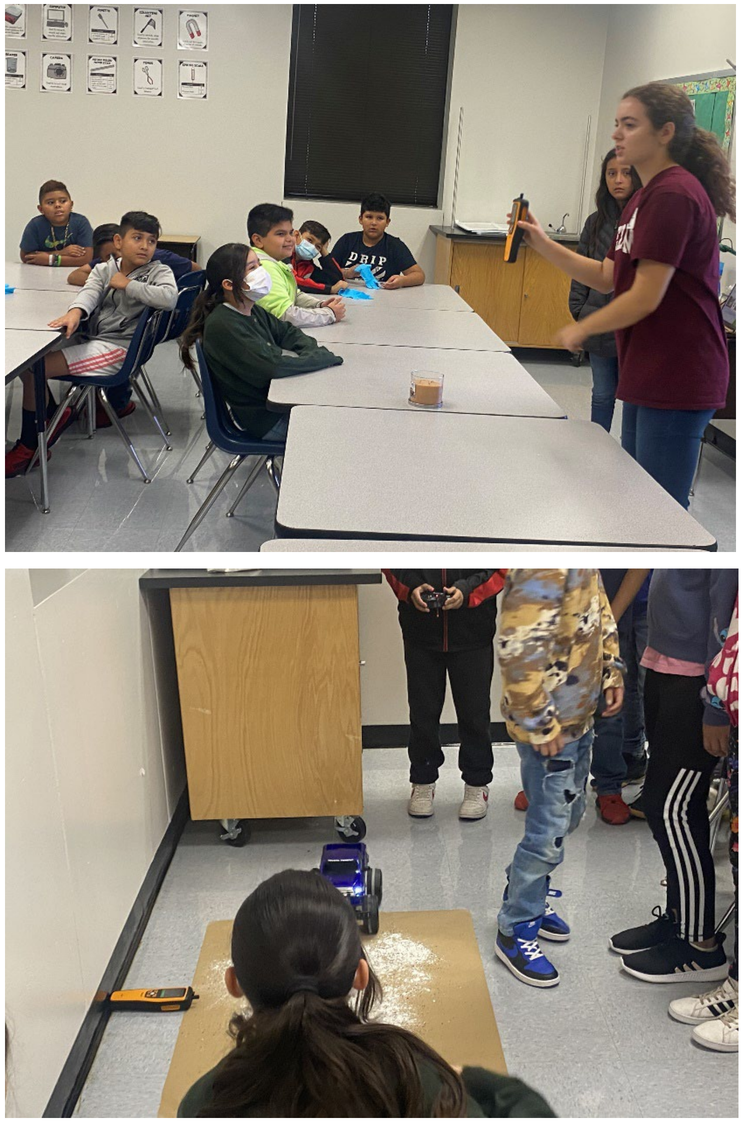

Figure 8. (Top panel) Undergraduate assistant Alyvia McEwen explains how to read the handheld PM monitor for the candle-burning demonstration. (Bottom panel) Volunteers drive the remote-controlled car over the flour patch as they visualize tires kicking up particles.

References

1. Grineski, S.E., S.E. Clark-Reyna, and T.W. Collins, *School-based exposure to hazardous air pollutants and grade point average: A multi-level study.* Environmental Research, 2016. **147**: p. 164-171.
2. Strife, S. and L. Downey, *Childhood Development and Access to Nature: A New Direction for Environmental Inequality Research.* Organization & Environment, 2009. **22**(1): p. 99-122.
3. Roth, S., *Air pollution, educational achievements, and human capital formation.* IZA World of Labor, 2017.
4. Brugge, D., J.L. Durant, and C. Rioux, *Near-highway pollutants in motor vehicle exhaust: a review of epidemiologic evidence of cardiac and pulmonary health risks.* Environ Health, 2007. **6**: p. 23.
5. Bateson, T.F. and J. Schwartz, *Children's response to air pollutants.* J Toxicol Environ Health A, 2008. **71**(3): p. 238-43.

6. Nopmongcol, U., W. Khamwichit, M.P. Fraser, and D.T. Allen, *Estimates of heterogeneous formation of secondary organic aerosol during a wood smoke episode in Houston, Texas.* Atmospheric Environment, 2007. **41**(14): p. 3057-3070.
7. III, C.A.P. and D.W. Dockery, *Health Effects of Fine Particulate Air Pollution: Lines that Connect.* Journal of the Air & Waste Management Association, 2006. **56**(6): p. 709-742.
8. Pererz, L., M. Medina-Ramon, N. Kunzli, A. Alastuey, J. Pey, N. Perez, R. Garcia, A. Tobias, X. Querol, and J. Sunyer, *Size Fractionate Particulate Matter, Vehicle Traffic, and Case-Specific Daily Mortality in Barcelona, Spain.* Environmental Science & Technology, 2009. **43**(13): p. 4707-4714.
9. Hays, M.D., S.H. Cho, R. Baldauf, J.J. Schauer, and M. Shaferd, *Particle size distributions of metal and non-metal elements in an urban near-highway environment.* Atmospheric Environment, 2011. **45**(4): p. 925-934.
10. Rauch, S., H.F. Hemond, B. Peucker-Ehrenbrink, K.H. Ek, and G.M. Morrison, *Platinum group element concentrations and osmium isotopic composition in urban airborne particles from Boston, Massachusetts.* Environmental Science & Technology, 2005. **39**(24): p. 9464-9470.
11. Sullivan, D.W., J.H. Price, B. Lambeth, K.A. Sheedy, K. Savanich, and R.J. Tropp, *Field study and source attribution for $PM_{2.5}$ and PM_{10} with resulting reduction in concentrations in the neighborhood north of the Houston Ship Channel based on voluntary efforts.* Journal of the Air & Waste Management Association, 2013. **63**(9): p. 1070-1082.
12. Bozlaker, A., J.M. Prospero, J. Price, and S. Chellam, *Identifying and Quantifying the Impacts of Advected North African Dust on the Concentration and Composition of Airborne Fine Particulate Matter in Houston and Galveston, Texas.* Journal of Geophysical Research: Atmospheres, 2019. **124**(22): p. 12282-12300.
13. Bozlaker, A., J.M. Prospero, M.P. Fraser, and S. Chellam, *Quantifying the contribution of long-range Saharan Dust transport on particulate matter concentrations in Houston, Texas, using detailed elemental analysis.* Environmental Science & Technology, 2013. **47**(18): p. 10179-10187.
14. Kulkarni, P., S. Chellam, and M.P. Fraser, *Tracking petroleum refinery emission events using Lanthanum and Lanthanides as elemental markers for $PM_{2.5}$.* Environmental Science & Technology, 2007. **41**(19): p. 6748-6754.
15. World Health Organization, *Prioritization of pathogens to guide discovery, research and development of new antibiotics for drug-resistant bacterial infections, including tuberculosis*. 2017, World Health Organization: Geneva.
16. World Health Organization, *WHO fungal priority pathogens list to guide research, development, and public health action*. 2022, World Health Organization: Geneva.
17. Polymenakou, P.N., M. Mandalakis, E.G. Stephanou, and A. Tselepides, *Particle size distribution of airborne microorganisms and pathogens during an Intense African dust event in the eastern Mediterranean.* Environmental Health Perspectives, 2008. **116**(3): p. 292-296.
18. Das, S., A. McEwen, J. Prospero, D. Spalink, and S. Chellam, *Respirable Metals, Bacteria, and Fungi during a Saharan–Sahelian Dust Event in Houston, Texas.* Environmental Science & Technology, 2023: p. DOI: 10.1021/acs.est.3c04158.
19. Kheirbek, I., J. Haney, S. Douglas, K. Ito, and T. Matte, *The Contribution of Motor Vehicle Emissions to Ambient Fine Particulate Matter Public Health Impacts in New York City: A Health Burden Assessment.* Environmental Health, 2016. **15**(1): p. 89.
20. Ghosh, R., F. Lurmann, L. Perez, B. Penfold, S. Brandt, J. Wilson, M. Milet, N. Künzli, and R. McConnell, *Near-Roadway Air Pollution and Coronary Heart Disease: Burden of Disease and Potential Impact of a Greenhouse Gas Reduction Strategy in Southern California.* Environmental Health Perspectives, 2016. **124**(2): p. 193-200.
21. Zhang, K. and S. Batterman, *Air Pollution and Health Risks Due to Vehicle Traffic.* Science of the Total Environment, 2013. **450-451**: p. 307-316.
22. Pateraki, S., M. Manousakas, K. Bairachtari, V. Kantarelou, K. Eleftheriadis, C. Vasilakos, V.D. Assimakopoulos, and T. Maggos, *The Traffic Signature on the Vertical PM Profile: Environmental and Health Risks Within an Urban Roadside Environment.* Science of The Total Environment, 2019. **646**: p. 448-459.
23. Brugge, D., J.L. Durant, and C. Rioux, *Near-highway pollutants in motor vehicle exhaust: A review of epidemiologic evidence of cardiac and pulmonary health risks.* Environmental Health, 2007. **6**: p. 1-13.

24. Shiraiwa, M., K. Ueda, A. Pozzer, G. Lammel, C.J. Kampf, A. Fushimi, S. Enami, A.M. Arangio, J. Frohlich-Nowoisky, Y. Fujitani, A. Furuyama, P.S.J. Lakey, J. Lelieveld, K. Lucas, Y. Morino, U. Poschl, S. Takaharna, A. Takami, H.J. Tong, B. Weber, A. Yoshino, and K. Sato, *Aerosol Health Effects from Molecular to Global Scales.* Environmental Science & Technology, 2017. **51**(23): p. 13545-13567.
25. Fuzzi, S., U. Baltensperger, K. Carslaw, S. Decesari, H. Denier van der Gon, M.C. Facchini, D. Fowler, I. Koren, B. Langford, U. Lohmann, E. Nemitz, S. Pandis, I. Riipinen, Y. Rudich, M. Schaap, J.G. Slowik, D.V. Spracklen, E. Vignati, M. Wild, M. Williams, and S. Gilardoni, *Particulate matter, air quality and climate: lessons learned and future needs.* Atmosperic Chemistry and Physics, 2015. **15**(14): p. 8217-8299.
26. Farahani, V.J., A. Altuwayjiri, M. Pirhadi, V. Verma, A.A. Ruprecht, E. Diapouli, K. Eleftheriadis, and C. Sioutas, *The oxidative potential of particulate matter (PM) in different regions around the world and its relation to air pollution sources.* Environmental Science: Atmospheres, 2022. **2**(5): p. 1076-1086.
27. Verma, V., C. Sioutas, and R.J. Weber. *Oxidative Properties of Ambient Particulate Matter - An Assessment of the Relative Contributions from Various Aerosol Components and Their Emission Sources*. in *Symposium on Multiphase Chemistry of Atmospheric Aerosols / Fall 2017 ACS Meeting*. 2017. Washington, DC.
28. Daellenbach, K.R., G. Uzu, J. Jiang, L.-E. Cassagnes, Z. Leni, A. Vlachou, G. Stefenelli, F. Canonaco, S. Weber, A. Segers, J.J.P. Kuenen, M. Schaap, O. Favez, A. Albinet, S. Aksoyoglu, J. Dommen, U. Baltensperger, M. Geiser, I. El Haddad, J.-L. Jaffrezo, and A.S.H. Prévôt, *Sources of particulate-matter air pollution and its oxidative potential in Europe.* Nature, 2020. **587**(7834): p. 414-419.
29. Eaves, L.A., H.T. Nguyen, J.E. Rager, K.G. Sexton, T. Howard, L. Smeester, A.N. Freedman, K.M. Aagaard, C. Shope, B. Lefer, J.H. Flynn, M.H. Erickson, R.C. Fry, and W. Vizuete, *Identifying the Transcriptional Response of Cancer and Inflammation-Related Genes in Lung Cells in Relation to Ambient Air Chemical Mixtures in Houston, Texas.* Environmental Science & Technology, 2020. **54**(21): p. 13807-13816.
30. Bruhl, R.J., S.H. Linder, and K. Sexton, *Case Study of Municipal Air Pollution Policies: Houston's Air Toxic Control Strategy under the White Administration, 2004-2009.* Environmental Science & Technology, 2013. **47**(9): p. 4022-4028.
31. Liu, Q.Y., J. Baumgartner, Y.X. Zhang, Y.J. Liu, Y.J. Sun, and M.G. Zhang, *Oxidative Potential and Inflammatory Impacts of Source Apportioned Ambient Air Pollution in Beijing.* Environmental Science & Technology, 2014. **48**(21): p. 12920-12929.
32. Abera, A., J. Friberg, C. Isaxon, M. Jerrett, E. Malmqvist, C. Sjöström, T. Taj, and A.M. Vargas, *Air Quality in Africa: Public Health Implications.* Annual Review of Public Health, 2021. **42**(1): p. 193-210.
33. Shakya, K.M., P. Louchouarn, and R.J. Griffin, *Lignin-Derived Phenols in Houston Aerosols: Implications for Natural Background Sources.* Environmental Science & Technology, 2011. **45**(19): p. 8268-8275.
34. Clark, A.E., S. Yoon, R.J. Sheesley, and S. Usenko, *Spatial and Temporal Distributions of Organophosphate Ester Concentrations from Atmospheric Particulate Matter Samples Collected across Houston, TX.* Environmental Science & Technology, 2017. **51**(8): p. 4239-4247.
35. Fröhlich-Nowoisky, J., C.J. Kampf, B. Weber, J.A. Huffman, C. Pöhlker, M.O. Andreae, N. Lang-Yona, S.M. Burrows, S.S. Gunthe, W. Elbert, H. Su, P. Hoor, E. Thines, T. Hoffmann, V.R. Després, and U. Pöschl, *Bioaerosols in the Earth system: Climate, health, and ecosystem interactions.* Atmospheric Research, 2016. **182**: p. 346-376.
36. Griffin, D.W., *Atmospheric movement of microorganisms in clouds of desert dust and implications for human health.* Clinical Microbiology Reviews, 2007. **20**(3): p. 459-477.
37. https://www.census.gov/quickfacts/fact/table/galenaparkcitytexas/INC110217. Accessed June 20, 2019.
38. Davidson, C.I., R.F. Phalen, and P.A. Solomon, *Airborne particulate matter and human health: A review.* Aerosol Science and Technology, 2005. **39**(8): p. 737-749.
39. Grineski, S.E. and T.W. Collins, *Geographic and social disparities in exposure to air neurotoxicants at U.S. public schools.* Environmental Research, 2018. **161**: p. 580-587.
40. Tessum, C.W., J.S. Apte, A.L. Goodkind, N.Z. Muller, K.A. Mullins, D.A. Paolella, S. Polasky, N.P. Springer, S.K. Thakrar, J.D. Marshall, and J.D. Hill, *Inequity in consumption of goods and services adds to racial–ethnic disparities in air pollution exposure.* Proceedings of the National Academy of Sciences, 2019. **116**(13): p. 6001-6006.
41. Bullard, R.D. and B.H. Wright, *ENVIRONMENTAL JUSTICE FOR ALL - COMMUNITY PERSPECTIVES ON HEALTH AND RESEARCH NEEDS.* Toxicology and Industrial Health, 1993. **9**(5): p. 821-841.

42. Bozlaker, A., J.M. Prospero, J. Price, and S. Chellam, *Linking Barbados mineral dust aerosols to North African sources using elemental composition and radiogenic Sr, Nd, and Pb Isotope signatures.* Journal of Geophysical Research: Atmospheres, 2018. **123**(2): p. 1384-1400.
43. Das, S., B.V. Miller, J. Prospero, and S. Chellam, *Sr-Nd-Hf isotopic analysis of reference materials and natural and anthropogenic particulate matter sources: Implications for accurately tracing North African dust in complex urban atmospheres.* Talanta, 2022. **241**: p. 123236.
44. Danadurai, K.S.K., S. Chellam, C.T. Lee, and M.P. Fraser, *Trace elemental analysis of airborne particulate matter using dynamic reaction cell inductively coupled plasma - mass spectrometry: application to monitoring episodic industrial emission events.* Analytica Chimica Acta, 2011. **686**(1-2): p. 40-49.
45. Bozlaker, A., B. Buzcu-Guven, M.P. Fraser, and S. Chellam, *Insights into PM_{10} sources in Houston, Texas: Role of petroleum refineries in enriching lanthanoid metals during episodic emission events.* Atmospheric Environment, 2013. **69**: p. 109-117.
46. Caporaso, J.G., J. Kuczynski, J. Stombaugh, K. Bittinger, F.D. Bushman, E.K. Costello, N. Fierer, A.G. Peña, J.K. Goodrich, J.I. Gordon, G.A. Huttley, S.T. Kelley, D. Knights, J.E. Koenig, R.E. Ley, C.A. Lozupone, D. McDonald, B.D. Muegge, M. Pirrung, J. Reeder, J.R. Sevinsky, P.J. Turnbaugh, W.A. Walters, J. Widmann, T. Yatsunenko, J. Zaneveld, and R. Knight, *QIIME allows analysis of high-throughput community sequencing data.* Nature Methods, 2010. **7**(5): p. 335-336.
47. Rognes, T., T. Flouri, B. Nichols, C. Quince, and F. Mahé, *VSEARCH: a versatile open source tool for metagenomics.* PeerJ, 2016. **4**: p. e2584.
48. Quast, C., E. Pruesse, P. Yilmaz, J. Gerken, T. Schweer, P. Yarza, J. Peplies, and F.O. Glöckner, *The SILVA ribosomal RNA gene database project: improved data processing and web-based tools.* Nucleic Acids Research, 2013. **41**(Database issue): p. D590-6.
49. Kõljalg, U., H.R. Nilsson, D. Schigel, L. Tedersoo, K.H. Larsson, T.W. May, A.F.S. Taylor, T.S. Jeppesen, T.G. Frøslev, B.D. Lindahl, K. Põldmaa, I. Saar, A. Suija, A. Savchenko, I. Yatsiuk, K. Adojaan, F. Ivanov, T. Piirmann, R. Pöhönen, A. Zirk, and K. Abarenkov, *The Taxon Hypothesis Paradigm-On the Unambiguous Detection and Communication of Taxa.* Microorganisms, 2020. **8**(12): p. 1910.
50. Watson, J.G., N.F. Robinson, J.C. Chow, R.C. Henry, B.M. Kim, T.G. Pace, E.L. Meyer, and Q. Nguyen, *The USEPA/DRI chemical mass balance receptor model, CMB 7.0.* Environmental Software, 1990. **5**(1): p. 38-49.
51. Das, S. and S. Chellam, *Estimating light-duty vehicles' contributions to ambient $PM_{2.5}$ and PM_{10} at a near-highway urban elementary school via elemental characterization emphasizing Rhodium, Palladium, and Platinum.* Science of the Total Environment, 2020. **747**: p. 141268.
52. Bozlaker, A., N.J. Spada, M.P. Fraser, and S. Chellam, *Elemental characterization of $PM_{2.5}$ and PM_{10} emitted from light duty vehicles in the Washburn tunnel of Houston, Texas: Release of rhodium, palladium, and platinum.* Environmental Science & Technology, 2014. **48**(1): p. 54-62.
53. Reff, A., P.V. Bhave, H. Simon, T.G. Pace, G.A. Pouliot, J.D. Mobley, and M. Houyoux, *Emissions inventory of $PM_{2.5}$ trace elements across the United States.* Environmental Science & Technology, 2009. **43**(15): p. 5790-5796.
54. Moreno, T., X. Querol, A. Alastuey, J. de la Rosa, A.M. Sánchez de la Campa, M. Minguillón, M. Pandolfi, Y. González-Castanedo, E. Monfort, and W. Gibbons, *Variations in vanadium, nickel and lanthanoid element concentrations in urban air.* Science of the Total Environment, 2010. **408**(20): p. 4569-4579.
55. Kulkarni, P., S. Chellam, and M.P. Fraser, *Lanthanum and lanthanides in atmospheric fine particles and their apportionment to refinery and petrochemical operations in Houston, TX.* Atmospheric Environment, 2006. **40**(3): p. 508-520.
56. Bozlaker, A., B. Buzcu-Güven, M.P. Fraser, and S. Chellam, *Insights into PM10 sources in Houston, Texas: Role of petroleum refineries in enriching lanthanoid metals during episodic emission events.* Atmospheric Environment, 2013. **69**: p. 109-117.
57. Sullivan, D.W., J.H. Price, B. Lambeth, K.A. Sheedy, K. Savanich, and R.J. Tropp, *Field study and source attribution for PM2.5 and PM10 with resulting reduction in concentrations in the neighborhood north of the Houston Ship Channel based on voluntary efforts.* Journal of the Air and Waste Management Association 2013. **63**(9): p. 1070-82.

58. Han, I., D. Richner, H. An Han, L. Hopkins, D. James, and E. Symanski, *Evaluation of metal aerosols in four communities adjacent to metal recyclers in Houston, Texas, USA.* J Air Waste Manag Assoc, 2020. **70**(5): p. 568-579.
59. Rodriguez-Arias, R.M., J. Rojo, F. Fernandez-Gonzalez, and R. Perez-Badia, *Desert dust intrusions and their incidence on airborne biological content. Review and case study in the Iberian Peninsula.* Environmental Pollution, 2023. **316**.
60. Chaturvedi, S. and I.P. Sarethy, *Major Habitats and Diversity of Thermophilic Fungi*, in *Extremophilic Fungi: Ecology, Physiology and Applications*, S. Sahay, Editor. 2022, Springer Nature Singapore: Singapore. p. 55-75.